

# Synthesis and Transport Properties of $\text{Nd}_{1-x}\text{Sr}_x\text{CoO}_3$ Composite Oxides

Yi Yun Yang

College of Electronic and Information Engineering, Ankang University, Ankang 725000, China  
 yangyiyun@aku.edu.cn

The synthesis and transport properties of  $\text{Nd}_{1-x}\text{Sr}_x\text{CoO}_3$  ( $x=0.30, 0.40, 0.50$ ) composite oxides are investigated in this paper. The cobaltites  $\text{Nd}_{1-x}\text{Sr}_x\text{CoO}_3$  ( $x=0.30, 0.40, 0.50$ ) samples were prepared in a high temperature by traditional solid state reaction method. The magnetic data show that the system has long range ferromagnetic order in high temperature. The Curie temperature  $T_C$  increases, the ferromagnetism rapidly increases, and the magnetic curve for  $x=0.50$  samples reaches the maximum. After the transition from paramagnetic to ferromagnetic phase, ferrimagnetic transition occurred at low temperature. Moreover, the transport properties show when Sr content increase, due to the hole introduce, the resistivity of system clearly decreases, reaching the minimum at  $x=0.5$ . The transition can be observed from the obvious insulator conductivity to the weak metal conductivity. The peaks of MR are close to the Curie temperature, the maximum is about 17.5%, and the peak value occurred about 175 K for  $x=0.50$ .

## 1. Introduction

The transport properties and magnetic studies under extreme conditions are one of the hot topics (Jiráček et al., 1985; Tsubouchi et al., 2002; Dho and Hur, 2006). Moreover, the research of magnetism has established the basic theoretical system, such as band theory, crystal field theory and coordination field theory. A number of models, such as double exchange model, were proposed. These are same as the results of existing magnetic experiment. Since Helmut et al. discovered the colossal magnetoresistance effect in  $\text{La}_{2/3}\text{Ba}_{1/3}\text{MnO}_3$  films (Helmut et al., 1993); the perovskite manganese oxide has been widely studied (Bindu et al., 2011; Anamitra et al., 2012). As a unique group closely related to manganese oxides, cobalt oxide also attracts people's attention (Señaris-Rodríguez and Goodenough, 1995; Paraskevopoulos et al., 2001). Cobaltites provide a unique opportunity for basic research on oxides (Davies et al., 2005). In recent years, the magnetoresistance (MR) was found for cobaltites. In 1995, the magnetoresistance effect was found in  $\text{La}_{1-x}\text{Sr}_x\text{CoO}_3$  thin film, and in 1997 magnetoresistance effect was found in the cobalt oxide  $\text{LaBaCo}_2\text{O}_{5.4}$  ( $L=\text{Eu}, \text{Gd}$ ) (Martin et al., 1997). Moreover, studies on CMR effect have found that the intrinsic phase separation plays an important role in understanding the physical characteristics of the system. Among them,  $\text{La}_{1-x}\text{Sr}_x\text{CoO}_3$  system is widely studied. Due to the change of the spin state of cobalt ion, the transformation of spin state not only influences magnetic characteristics, but also influences the electrical transport properties of the system.  $\text{La}_{1-x}\text{Sr}_x\text{CoO}_3$  system exist phase separation, that is, the ferromagnetic region is in the non-magnetic basement, and the spin glass is located between the ferromagnetic cluster and the non-magnetic field, forming the spin glass interface layer of the ferromagnetic cluster (Wu and Leighton, 2003; Uddin et al., 2017; Saron et al., 2016; Yang, 2017; Jubsilp et al., 2018). The study of spin glass system plays an important role in the further study of CMR phenomenon. Research on cobaltites system is still lags behind that of the manganese oxide. In order to better understand the cobalt oxide system, it is important to further research cobaltites system.

In this paper, magnetoresistance (MR) effect and transport properties of  $\text{Nd}_{1-x}\text{Sr}_x\text{CoO}_3$  ( $x=0.30, 0.40, 0.50$ ) were studied systematically. Dc magnetic data show that the system has long range ferromagnetic order in high temperature. The ferromagnetic properties were further determined, because the peak of ac susceptibility appears near  $T_C$ . Transport characteristics show the transition from insulator to metal.

## 2. Experiments

### 2.1 Materials

The raw materials adopt the ideal ratio of  $\text{Co}_2\text{O}_3$ ,  $\text{Nd}_2\text{O}_3$  and  $\text{SrCO}_3$ . In order to remove the moisture in the oxide  $\text{Nd}_2\text{O}_3$ , the thermal weight-differential thermal analysis (TG-DTA) test was performed before the sample preparation. Test conditions are  $10^\circ\text{C} \sim 1100^\circ\text{C}$  in the air,  $10^\circ\text{C}/\text{min}$ .

### 2.2 Synthesis of samples

TG-DTA test results show obvious peak in the two places of  $280^\circ\text{C}$  and  $420^\circ\text{C}$ . And the quality of  $\text{Nd}_2\text{O}_3$  does not change after  $900^\circ\text{C}$ . As a result, the  $\text{Nd}_2\text{O}_3$  was precalcined 4 h in  $900^\circ\text{C}$ , for getting rid of some water and other gases.  $\text{Nd}_{1-x}\text{Sr}_x\text{CoO}_3$  (NSCO) was made by solid reaction method. Under the pressure of 8 MPa, it is pressed into a circle piece. These pieces are about thickness of 1mm with the radius of 6.5mm, which were fired in the air.

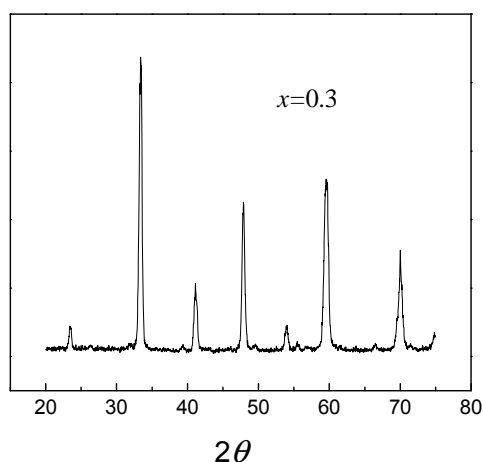


Figure 1: The X-ray diffraction patterns of perovskite cobaltites  $\text{Nd}_{0.70}\text{Sr}_{0.30}\text{CoO}_3$

### 2.3 Characterization techniques

The X-ray diffraction pattern was tested using the Bede D<sup>1</sup> XRD spectrometer. Wavelength was 0.15406 nm. Scan step were  $0.02^\circ$  and scan range is  $20^\circ \sim 75^\circ$ . Figure 1 shows a single phase of the sample with  $a \leq c/\sqrt{2} \leq b$ . The test of magnetoresistance effect and transport characteristics was made by the Physics Property Measurement System.

## 3. Results and discussion

### 3.1 Dc magnetization and ac susceptibility

Figure 2 is field cooled (FC) magnetization for  $\text{Nd}_{1-x}\text{Sr}_x\text{CoO}_3$  ( $x=0.30, 0.40, 0.50$ ) samples, that is  $M(T)$  curve. The test temperature condition is from 5K to 300K, dc magnetic field is 1,000 Oe.

Low doping samples of NSCO ( $x < 0.20$ ) are spin glass (SG) state, that is, the short-range ferromagnetic (FM) particles is in the non-magnetic insulation basement. The ferromagnetic order was located in the insulation basement which formed the magnetic moment disordered interface layer or surface layer. The spin glass phase is likely to be in the interface layer between FM cluster and non-magnetic insulation substrate. The NSCO system has an inherent phase separation, and some literatures give a phase diagram of the NSCO system (Fondado et al., 2001; Stauffer and Leighton, 2004). When  $x < 0.20$ , NSCO is spin glass phase, but  $0.20 < x \leq 0.50$  NSCO is characterized by ferromagnetic order.

In Figure 2, all curves present ferromagnetic order characteristics and the value of  $M(T)$  increases clearly near the Curie temperature  $T_C$ . With the increase of doping, the  $\text{Co}^{4+}$  ions increase, the double exchange function was enhanced, the size and number of ferromagnetic particles increase, so that the  $x \geq 0.3$  system shows ferromagnetic order characteristics in high doping. Under field cooled condition, the spin of the ferromagnetic cluster was consistent with the orientation of the external field, causing the large magnetization to appear near  $T_C$ . As is shown in Figure 2 the Curie temperature  $T_C$  of the three samples ( $x=0.30, 0.40, 0.50$ ) respectively is

145.7 K, 169.2K and 175.5 K. With the increase of  $x$ , the  $T_C$  increases, the ferromagnetic properties clearly increase, and the magnetic curve for  $x=0.5$  samples reaches the maximum.

Near the Curie temperature  $T_C$  in the  $M(T)$  curve, ferromagnetic behavior appears, but at low temperature, the magnetization shows a decreasing trend. After the transition from paramagnetic to ferromagnetic phase, ferrimagnetic transition occurred at low temperature. The experiment results of neutron diffraction showed that the decrease of magnetization for NSCO system which was caused by ferromagnetic order at low temperature (Krimmel et al., 2001). The reason is due to the antiparallel arrangement of cobalt ions and neodymium ions, that is, the anti-ferromagnetic coupling of  $\text{Nd}^{3+}$  and  $\text{Co}^{3+}/\text{Co}^{4+}$  magnetic moment. Since the exchange function between neodymium ions and cobalt ions is not strong, the ferrimagnetic transition occurs at low temperature. As can be seen from the magnetization curve, as  $x$  increases, the temperature of ferrimagnetic order  $T_{\text{Ferr}}$  increases. The coupling effect between  $\text{Nd}^{3+}$  and  $\text{Co}^{3+}/\text{Co}^{4+}$  increased with the increase of doping Sr, so the temperature of ferrimagnetic transition  $T_{\text{Ferr}}$  appeared at higher temperature.

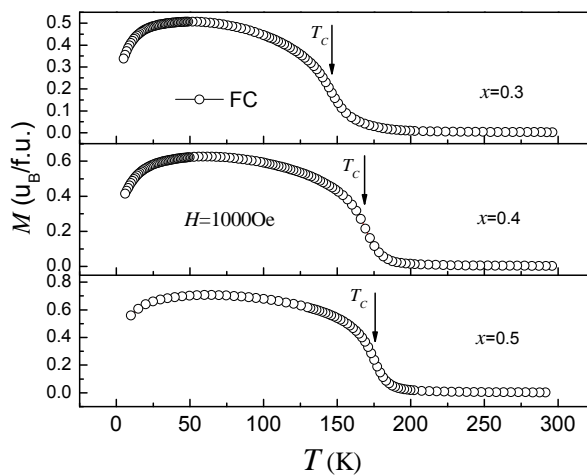


Figure 2: Field cooled magnetization of perovskite cobaltites  $\text{Nd}_{1-x}\text{Sr}_x\text{CoO}_3$  ( $x=0.30, 0.40, \text{ and } 0.50$ )

For  $x=0.30, 0.40, 0.50$  samples, the peak value of susceptibility occurred about 144 K, 169 K and 175 K respectively. The peak value is near the Curie temperature  $T_C$ , and the peak value does not change with the frequency, indicating that the  $\chi'(T)$  is the same as the test data of  $M(T)$  curve. From the  $\chi'(T)$ , samples showed the ferromagnetic behavior as we expected.

When the doping  $x$  increases, the ac susceptibility of the sample gradually increases. This is same as the test results of the  $M(T)$  curve. When doping Sr increase, the size and number of the cluster increases and the ferromagnetism of samples increases. The relation between the imaginary components and the measurement frequency show the  $\chi''(T)$  (not shown) also increases significantly with increasing  $x$  content. The peak temperature of  $\chi''(T)$  of the sample is lower than the peak temperature of  $\chi'(T)$ , but they are very close. This result is consistent with the results of  $\text{La}_{1-x}\text{Sr}_x\text{CoO}_3$  system.

### 3.2 Resistivity and magnetoresistance

The carrier in metal and semiconductor will be directed motion in the field, but they will also be scattered by impurities and lattice vibrations (Zhou et al., 1997; Zhou and Goodenough, 1998). Multiple factors compete with each other and eventually reach equilibrium, thus forming a steady state transport mechanism. In the zero magnetic fields, we carried out the electrical transport property test by using the four-electrode method in the range of 10 K ~300 K. The curve of the resistivity  $\rho(T)$  for  $\text{Nd}_{0.70}\text{Sr}_{0.30}\text{CoO}_3$  sample is presented in the figure.

We can see from the Figure 3, there is no insulator-metal (IM) transition in curve throughout the test range.  $d\rho/dT < 0$ , it is always the semiconductor property, i.e. the  $\rho$  increases when the temperature decrease. In Figure 3, the curve of the conductivity  $\sigma(T)$  for  $x=0.30$  was given. This sample is near vicinity of insulator-metal transition. When the temperature is approximately zero, the conductivity is about zero.

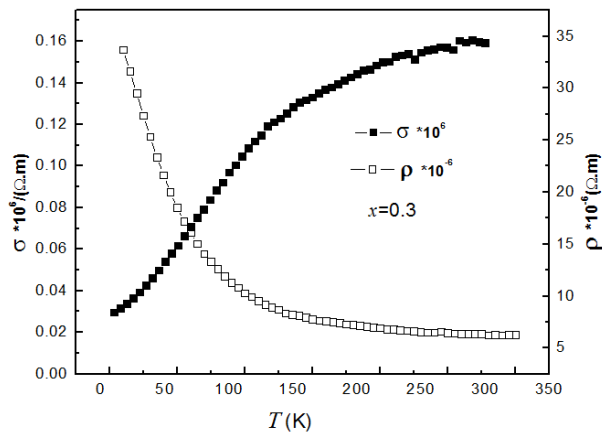


Figure 3: The curves of the resistivity and the conductivity of  $Nd_{0.70}Sr_{0.30}CoO_3$

In the cobaltites system, with the increase of  $Co^{4+}$  content, the Mott variable range hopping (VRH) becomes the main mechanism of conduction (Shafarman et al., 1989; Ziese, 2001):

$$\rho(T) = \rho_0 \exp[(T_0 / T)^{1/4}] \quad (1)$$

In the equation,  $T_0$  is the characteristics of temperature, and  $\rho_0$  is its resistivity. Figure 4 shows the fitting results of experimental data with VRH model.

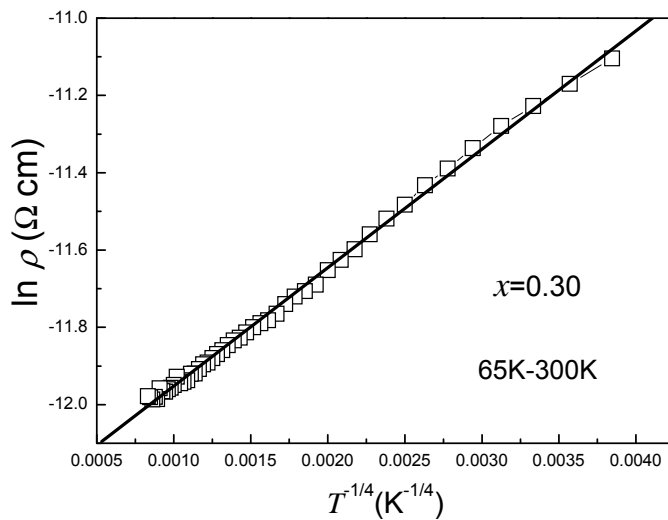


Figure 4: Temperature dependence of the resistivity of  $Nd_{0.70}Sr_{0.30}CoO_3$  shows that the best fit was the VRH

In Figure 4, when the relationship between resistivity and temperature is converted to  $\ln \rho - T^{-1/4}$ , the curve of the resistivity shows that the best fit with the VRH. The results are the similar to those obtained in the literature (Li et al., 2016).

In Figure 5 show the electrical transport behavior for  $Nd_{1-x}Sr_xCoO_3$  ( $x=0.30, 0.40, 0.50$ ) in more detail. The  $x=0.30$  sample is exhibited the conductive property of the semiconductor. It can be seen that low doping sample resistivity is relatively large. When Sr content increase, due to the hole introduce, the resistivity of NSCO clearly decreases, reaching the minimum at  $x=0.5$ . As the doping  $x$  content increases, we can observe that the transition from the obvious insulator conductivity to the weak metal conductivity. For  $x=0.40$  sample, there was an insulator- metal (IM) transition near  $T_c$ , but the  $\rho(T)$  for  $x=0.50$  was metal conductivity

The inset of Figure 5 shows the MR (T) curve of the sample  $x=0.50$ . In the region dominated by ferromagnetism the system exhibits metallic behavior and CMR in the vicinity of  $T_c$ , as show in Figure 5. Generally, the magnitude of the magnetoresistance effect defined as:

$$MR = (\rho(0) - \rho(H)) / \rho(0) \times 100\% \quad (2)$$

Where  $\rho(H)$  is the resistivity of the material when the external magnetic field is  $H=5$  kOe, and  $\rho(0)$  is the resistivity of zero field. The peak of MR was near the Curie temperature, the peak value occurred in about 175K. In the  $H=5$ kOe field, the MR value is about 17.5%, which is same as the  $\text{La}_{1-x}\text{Sr}_x\text{CoO}_3$  system.

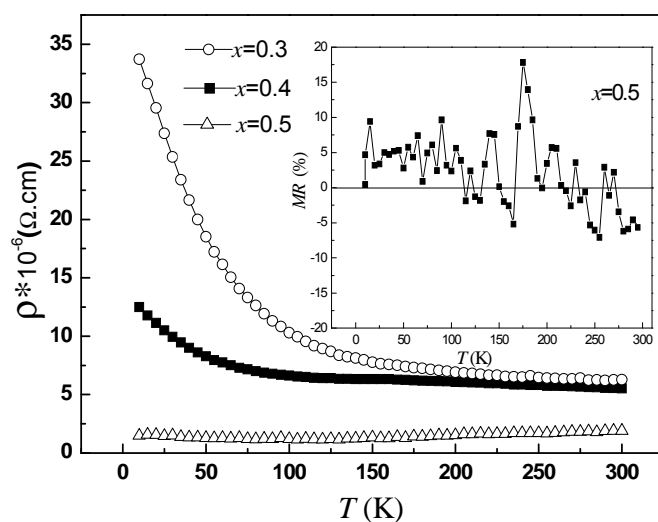


Figure 5: Temperature dependence of the resistivity of  $\text{Nd}_{1-x}\text{Sr}_x\text{CoO}_3$ . Inset shows temperature dependence of the magnetoresistance, for  $x=0.50$

#### 4. Conclusions

In summary, the synthesis and transport characteristics of  $\text{Nd}_{1-x}\text{Sr}_x\text{CoO}_3$  ( $x=0.30, 0.40, 0.50$ ) composite oxides are investigated in detail. The magnetization results presented that with the increase of  $x$ , the Curie temperature  $T_C$  increases, the ferromagnetism clearly increases, and the  $M(T)$  curve of  $x=0.5$  samples reaches the maximum. The long range ferromagnetic order appeared in the high temperature. Furthermore, the transport properties show when Sr content increase, due to the hole introduce, the resistivity of NSCO clearly decreases, reaching the minimum at  $x=0.5$ . We can observe that the transition from the obvious insulator conductivity to the weak metal conductivity. For  $x=0.4$  sample, there was an insulator- metal (IM) transition near  $T_C$ . The peak of MR was near the Curie temperature, the peak value occurred about 175 K for  $x=0.50$ . In the  $H=5$  kOe field, the MR value is about 17.5%.

#### Acknowledgments

The work is supported by the Special Scientific Research Program Funded of Ankang University (Program No.2015AYPYZR05), Project from Scientific Research Fund of Shaanxi Provincial Education Department (Grant No. 16JK1015).

#### References

- Anamitra M., William S.C., Nandini T., 2012, Strain controlled colossal magnetoresisit in magnganite thin films, *Condensed Matter*, 129, 3-5.
- Bindu R., Ganesh A., Kalobaran M., 2011, Signature of phase coexistence in electron doped manganite, *Journal of Physics: Conference Series*, 273, 40-43, DOI: 10.1088/1742-6596/273/1/012140
- Davies J.E., Wu J., Leighton C., Liu K., 2005, Magnetization Reveral and Nanoscopic Magnetic-Phase Separation in  $\text{La}_{1-x}\text{Sr}_x\text{CoO}_3$ , *Phys. Rev. B.*, 72, 134419-1-134419-2.
- Dho J., Hur N.H., 2006, Stabilization of Antiferromagnetic Phases by Magnetic Field Annealing in Phase Separated Manganites  $\text{Pr}_{1-x}\text{Ca}_x\text{MnO}_3$ , *Solid State Commun*, 140, 469-473, DOI: 10.1016/j.ssc.2006.08.050
- Fondado A., Breijo M.P., Rey-Cabezudo C., Sánchez-Andújar M., Mira J., Rivas J., Señarís-Rodríguez M.A., 2001, Synthesis, Characterization, Magnetism and Transport Properties of  $\text{Nd}_{1-x}\text{Sr}_x\text{CoO}_3$  Perovskites. *J. Alloys Comp.*, 324, 444-447, DOI: 10.1016/s0925-8388(01)01083-0

- Helmolt R.V., Wecker J., Holzapfel B., 1993, Giant Negative Magnetoresistance in Perovskite  $\text{La}_{3/2}\text{Ba}_{1/3}\text{MnO}_3$  Ferromagnetic Films, *Phys. Rev. Lett.*, 71, 2331-2333, DOI: 10.1103/PhysRevLett.71.2331
- Jiráček Z., Krupička S., Šimša Z., 1985, Neutron Diffraction Study  $\text{Pr}_{1-x}\text{Ca}_x\text{MnO}_3$  Perovskites, *J. Magn. Magn. Mater.* 53, 153-166, DOI: 10.1016/0304-8853(85)90144-1
- Jubsilp C., Rimdusit S., Takeichi T., 2018, Thermal stability and thermo-mechanical properties of nanoalumina-filled poly(benzoxazine-ester) composite films, *Chemical Engineering Transactions*, 70, 439-444, DOI: 10.3303/CET1870074
- Krimmel A., Reehuis M., Paraskevopoulos M., Hemberger J., Loidl A., 2001, Ferrimagnetic Behavior of  $\text{Nd}_{0.67}\text{Sr}_{0.33}\text{CoO}_3$ , *Phys. Rev. B.*, 64, 224404-1-224404-3.
- Li Y., Zhang Y.X., Kong X.R., Ding Y.P., Zhang R.Z., Tang J.Y. 2016, Thermal stability of the  $\text{Mg}_2\text{Ni}$ -based hydrogen storage alloy doped Ti element, *International Journal of Heat and Technology*, 34, 245-250. DOI: 10.18280/ijht.340213.
- Martin C., Maignan A., Pelloquin D., Nguyen N., Raveau B., 1997, Magneto-resistance in the Oxygen Deficient  $\text{LnBaCo}_2\text{O}_{5.4}$ , *Appl. Phys. Lett.*, 71, 1421-1422.
- Paraskevopoulos M., Hemberger J., Krimmel A., Loidl A., 2001, Magnetic Ordering and Spin-State Transition in  $\text{R}_{0.67}\text{Sr}_{0.33}\text{CoO}_3$ , *Phys. Rev. B.*, 63, 224416-1-224416-5.
- Saron M., Ponticorvo E., Cirillo C., Ciambelli P., 2016, Magnetic nanoparticles for pahn solid phase extraction, *Chemical Engineering Transactions*, 47, 313-318, DOI: 10.3303/CET1647053.
- Señaris-Rodríguez M.A., Goodenough J.B., 1995, Magnetic and Transport Properties of the System  $\text{La}_{1-x}\text{Sr}_x\text{CoO}_{3-\delta}$  ( $0 < x \leq 0.50$ ), *J. Solid State Chem*, 118, 323-325.
- Shafarman W.N., Koon D.W., Castner T.G., 1989, Dc conductivity of arsenic-doped silicon near the metal-insulator transition. *Phys. Rev. B.*, 40, 1216-1220.
- Stauffer D.D., Leighton C., 2004, Magnetic Phase Behavior of the Ferrimagnetic Doped Cobaltite  $\text{Nd}_{1-x}\text{Sr}_x\text{CoO}_3$ , *Phys. Rev. B.*, 70, 214414-2-214414-6.
- Tsubouchi S., Kyomen T., Itoh M., Gangly P., Oguni M., Shimojo Y., Mori Y., Yishii M., 2002, Simultaneous Metal-Insulator and Spin-State Transition in  $\text{Pr}_{0.5}\text{Ca}_{0.5}\text{CoO}_3$ , *Phys. Rev. B.*, 66, 052418-2-052418-6, DOI: 10.1103/PhysRevB.66.052418
- Uddin M.J., Halim M.A., Shalauddin M.M, 2017, Copper oxide-water nanofluid flow within an annulus shaped cavity: A numerical study on natural convective heat transfer, *Annales de Chimie - Science des Matériaux*, 41, 239-260, DOI: 10.3166/ACSM.41.239-260
- Wu J., Leighton C., 2003, Glassy Ferromagnetism and Magnetic Phase Separation in  $\text{La}_{1-x}\text{Sr}_x\text{CoO}_3$ , *Phys. Rev. B.*, 67, 174408-1-174408-10.
- Yang Y.Y., 2017, Investigation of the ferrimagnetic transition in doped cobaltite  $\text{Nd}_{1-x}\text{Sr}_x\text{CoO}_3$  ( $0.1 \leq x \leq 0.5$ ), *Chemical Engineering Transactions*, 59, 961-966, DOI: 10.3303/CET1759161.
- Zhou J.S., Goodenough J.B., Asamitsu A., Tokura Y., 1997, Pressure-Induced Polaronic to Itinerant Electronic Transition in  $\text{La}_{1-2x}\text{Sr}_x\text{MnO}_3$ , *Crystals. Phys. Rev. Lett.*, 79, 3234-3237, DOI: 10.1103/PhysRevLett.79.3234
- Zhou J.S., Goodenough J.B., 1998, Phonon-Assisted Double Exchange in Perovskite Manganites. *Phys. Rev. Lett.*, 80, 2665-2668, DOI: 10.1103/PhysRevLett.80.2665
- Ziese M., 2002, Extrinsic Magnetotransport Phenomena in Ferromagnetic Oxides, *Rep. Prog. Phys.*, 65, 143-249.